U. Walzer, R. Hendel, and J. Baumgardner. Variation of non-dimensional numbers and a thermal evolution model of the Earth's mantle. In E. Krause and W. Jäger, editors, High Perf. Comp. Sci. Engng. '02, pages 89-103. Berlin, 2003a.

Variation of non-dimensional numbers and a thermal evolution model of the Earth's mantle

Uwe Walzer[1], **Roland Hendel**[1], **John Baumgardner**[2]

[1] *Institut für Geowissenschaften, Friedrich-Schiller-Universität, Burgweg 11, 07749 Jena, Germany*
[2] *Los Alamos National Laboratory, MS B216 T-3, Los Alamos, NM 87545, USA*

Abstract. A 3-D compressible spherical-shell model of the thermal convection in the Earth's mantle has been investigated with respect to its long-range behavior. In this way, it is possible to describe the thermal evolution of the Earth more realistically than by parameterized convection models. The model is heated mainly from within by a temporally declining heat generation rate per volume and, to a minor degree, from below. The volumetrically averaged temperature, T_a, diminishes as a function of time, as in the real Earth. Therefore, the temperature at the core-mantle boundary, $T_{CMB,av}$, has not been kept constant but the heat flow, in accord with Stacey (1992). Therefore, $T_{CMB,av}$ decreases like T_a. This procedure seems to be reasonable since evidently nobody is able to propose a comprehensible thermostatic mechanism for CMB. First of all, a radial distribution of the starting viscosity has been derived using PREM and solid-state physics. The time dependence of the viscosity is essential for the evolution of the Earth since the viscosity rises with declining temperature. For numerical reasons, the temperature-dependent factor of the model viscosity is limited to four orders of magnitude.

The focus of this paper is an investigation of the variation of parameters, especially of the non-dimensional numbers as the Rayleigh number, Ra, the Nusselt number, Nu, the reciprocal value of the Urey number, Ror, the viscosity level, r_n, etc. For $0.0 \leq r_n \leq +0.3$, the authors arrived at Earth-like models. This interval contains the starting model. The quantification of the essential features of the model is provided by eight plots. Numerical procedure: The differential equations are solved using a fast multigrid solver and a second-order Runge-Kutta procedure with a FE method. On 128 processors, runs with 10649730 grid points need about 50 hours. Fig. 11 shows the scaling degree of our code.

If the temperature dependence of the viscosity, Eq. (4), is replaced by Eq. (10) then, in the interval $0.0 \leq r_n \leq +0.3$, reticularly connected thin cold sheet-like downwellings are found from the surface down to 1350 km depth. However, the movements along the upper surface are not plate-like.

1 Introduction

This paper presents a new thermal evolution model of the Earth's mantle. It is based on the assumption of thermal convection in a compressible spherical shell heated from within, for the most part. The focus is the variation of dimensionless parameters in order to show the reliability of the model.

The construction of this introduction results from the first paragraph. Here, some essential papers of other authors are reviewed. The main sources of the internal heating of the Earth stem from the transformation of kinetic energy of the parential bodies into heat during accretion (Safronov, 1972) and from the decay of radioactive elements with long half-life periods. Spohn and Schubert (1991) demonstrated that, after an early impact of a Mars-sized body, the Earth needs 1-10 Ma to come to equilibrium. Using such a starting point, Schubert et al. (1979, 1980) calculated the thermal evolution in a parameterized model where, from the integration of the energy conservation in the Earth's mantle, it follows that

$$Mc\frac{\partial T_a}{\partial t} = MH_0e^{-\lambda t} - Aq \tag{1}$$

where M is the mass of the mantle, c the specific heat, T_a the volume-averaged temperature of the mantle, H_0 the specific radiogenic heat generation rate at the beginning of mantle evolution, λ a unified rate constant, A the magnitude of the Earth's surface and q the mean mantle heat flow at the surface. According to the presumed heating mode, different Nu-Ra relations are used in these and the subsequently mentioned papers. Christensen (1984, 1985) studied the influence of a strongly temperature-dependent viscosity on thermal convection. Dependent on the assumed degree of temperature dependence of the viscosity, Christensen (1985), Solomatov (1995) and Reese et al. (1999) arrived at three different convection modes, a first regime with low temperature influence and movable upper boundary layer, the sluggish-lid regime and the stagnant-lid regime. For each regime, a different Nu-Ra relation has been derived.

Our evolution model of the mantle is a convective spherical-shell model, since the balance equations of energy, momentum and mass and later on also the balance equations of the sums of the number of the atoms of radioactive parent nuclides and the corresponding radiogenic daughter nuclides can be more realistically formulated for a spherical shell. Furthermore, the compressibility and associated effects such as viscous heating and adiabatic heating are relevant for the larger terrestrial planets (Earth, Venus). Therefore, these effects are taken into account in our model. For that reason, some papers of other authors are discussed here which show similar features. Bercovici et al. (1992) calculated compressible-fluid convection using the anelastic liquid approximation (ALA). The material parameters are supposed to be constants, expect the density $\rho(r)$. So, also the viscosity, η, is constant. The superadiabatic temperature difference, ΔT_{sa}, between the upper and the lower surface of the spherical shell is kept constant, too. The model has no internal heating. T_{bot} is the temperature at the lower surface, Di is the dissipation number, Ra_a is the Rayleigh number.

$$Ra_a = \left\langle \rho\alpha g h^3 \Delta T_{sa}/\eta\kappa \right\rangle \tag{2}$$

where α is the coefficient of thermal expansion, g gravity, h the depth of the mantle and κ the thermal diffusivity. $\langle\rangle$ denotes the volume-averaged value. In order to investigate compressibility effects, Ra_a, $\overline{Di}$ and $\overline{T}_{bot}/\Delta T_{sa}$ have been systematically varied. The thickness of the upper stagnant layer grows with rising $\overline{T}_{bot}/\Delta T_{sa}$. The model by Zhang and Yuen (1996) is somewhat more complex and resembles more to the mantle. ALA is used, too, but additionally the assumption

$$\tilde{\alpha}/\tilde{\gamma} = \tilde{\rho}_{ref}^{-2} \tag{3}$$

where the curly overbar denotes non-dimensional quantities; γ is the Gruneisen parameter and ρ_{ref} is a depth-dependent reference density using the Adams-Williamson equation. $\tilde{\alpha}$, $\tilde{\rho}_{ref}$, the thermal conductivity, $\tilde{k}$, and the reference temperature, $\tilde{T}_{ref}$, are weakly depth-dependent, $\tilde{\eta}$ is moderately depth-dependent. The number and the strength of plumes and subducting zones strongly depend on the depth dependence of the viscosity. Using other viscosity-depth relations, we can corroborate this experience. Viscous dissipation is maximum near the upper and lower surface of the spherical shell. Zhang and Yuen (1996) concluded that adiabatic and viscous heating increase each other in downwellings whereas viscous heating retards adiabatic cooling in plumes. For incompressible convection, this asymmetry causes a rising temperature in the interior of the shell.

2 Our model

In this paper, we investigate the effects of a systematic variation of non-dimensional parameters on our model. On the one hand, we used non-dimensional numbers which are fixed for one run, namely the Rayleigh numbers, $Ra(1)$ and $Ra(2)$, the Nusselt numbers, $Nu(1)$ and $Nu(2)$, the reciprocal values of the Urey numbers, $Ror(1)$ and $Ror(2)$, and a non-dimensional number, r_n, which characterizes the level of the viscosity profile. Below, these numbers will be defined. On the other hand, there are also time-dependent non-dimensional quantities, $Ra(t)$, $Nu(t)$ and $Ror(t)$, since the Earth's mantle as well as our model irreversibly evolve.

We calculate the thermal convection in a spherical shell with a ratio of the radii as in the Earth's mantle according to PREM, with an infinite Prandtl number, with impermeable free-slip boundaries, with a spatially homogeneous internal heating, subsiding as a function of time. The abundances of ^{238}U, ^{235}U, ^{232}Th and ^{40}K of the bulk silicate Earth are taken from McCulloch and Bennett (1994). These abundances deviate only slightly from those of the primitive mantle according to Hofmann (1988). The decay of the heat generation is an essential feature of the evolution of the mantle and must not be neglected. The primordial heat of the mantle is introduced by an initial adiabatic temperature distribution which is 3900 K at the core-mantle boundary (CMB) in our model. The upper surface temperature is thought to be constant at 288 K, constant with respect to time and space. Even if only

the primordial heat would exist, the thermal history of the mantle would be a decline in temperature. Radioactive decay, heat conduction and viscous dissipation are irreversible processes. Therefore, neither in this relatively simple model nor in the real mantle, steady states will occur during the considered time span of evolution. The non-dimensional numbers mentioned at the beginning make us independent of the details of the dimensional quantities which can be found in Walzer et al. (2002a). Furthermore, the model is compressible and takes into account the adiabatic and viscous heating. There are no continents in the model. So, the boundary conditions at the upper surface are equal everywhere. Moreover, the model does not contain chemical differentiation (Walzer and Hendel, 1999; Ogawa, 2000; DeSmet et al., 2000) and convective mixing of chemical reservoirs (Schmalzl, 1996). Similar to the model of Zhang and Yuen (1996), our method contains some quantities which weakly depend on the radius, r: The Figs. 1 and 2 by Walzer et al. (2002a) show the pressure, P, the reference density, ρ_{ref}, the bulk modulus, K, the Grueneisen parameter, γ, the thermal expansion coefficient, α, the specific heat at constant pressure, c_p, and the specific heat at constant volume, c_v, as a function of the radius, r. The coefficient α stems from Chopelas and Boehler (1992) and some related papers wheras the rest of the quantities have been derived from PREM and some usual solid-state physics formulae. The thermal conductivity, k, of the model is identical with that of Bercovici et al. (1992). A number of viscosity distributions is essential for the model. The P,T-dependence of the viscosity as well as the mineralogical phase boundaries at 410 and 660 km depth are reflected in these distributions. The basic distribution of the viscosity, η, results from

$$\eta(r) = 10^{r_n} \cdot \eta_1(r) \cdot exp\left[\frac{c_1}{T_{av}/T_{00}+1} - \frac{c_1}{2}\right] \tag{4}$$

for $r_n = 0$ where $\eta_1(r)$ is shown by Fig.1 and derived by Walzer and Hendel (2002) and Walzer et al. (2002a) using the seismological model PREM and solid-state physics.

The overall features of $\eta_1(r)$ show a certain resemblance with the viscosity profile according to Forte and Mitrovica (2002, their Fig. 2) and Ekström and Dziewonski (1998) although that profile has been derived by a totally different method. The latter method used density anomalies in the mantle and a simplified distribution of observed plate velocities given by the NUVEL–1 model. The mentioned density anomalies are derived from the observed shear-velocity anomalies and the observed free-air gravity anomalies which are calculated using the non-hydrostatic geopotential derived from satellite data.

The quantity r_n in Eq. (4) denotes a non-dimensional real number which characterizes the general level of the viscosity profile. In the third factor of Eq. (4), $c_1 = 9.2103$, $T_{00} = 1500\,\mathrm{K}$ and T_{av} is the laterally averaged temperature (in Kelvin) which is a function of the time, t, too. So, it is guaranteed that the temperature-dependent factor of the viscosity varies only in a range of

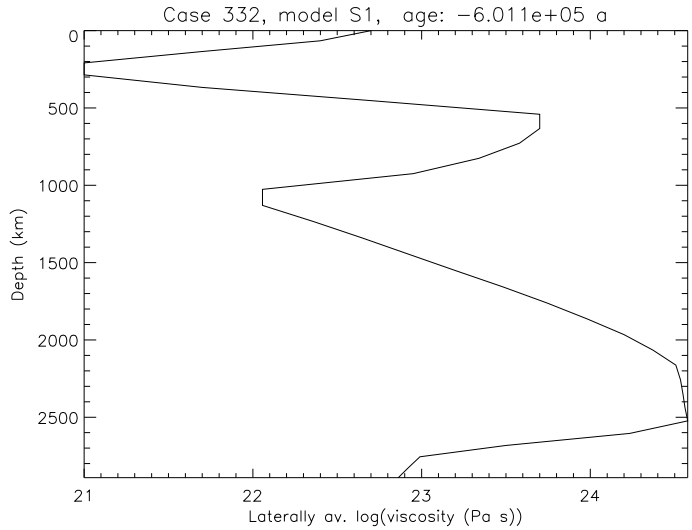

Fig. 1: Basic viscosity, $\eta_1(r)$, of the mantle as a function of depth, according to Walzer et al. (2002a).

four orders of magnitude. This assumption does not essentially distort the physics of the problem but, so, numerical problems are avoided.

Using our model, we want to calculate the last 4990 Ma of the thermal evolution of the mantle. This is the time after the formation of the Earth's core. So, not only some 100 Ma are relevant for our considerations.

a) *It is an essential feature of the evolution of the Earth, that its direction is defined by irreversible processes,* especially that the heat generation rate per volume, Q, decreases with time and that the Earth cools down, i.e. that the volume-averaged temperature, T_a, diminishes. The latter process would happen also if the internal heating would take place only at the beginning by accretion. From investigations of komatiites, it is well known that the temperature of the upper part of the mantle grows less by about 100 K per 10^9 a.

b) From geochemistry, it is well-known that the radioactive elements are concentrated mainly in the silicate shell but not in the metallic Earth's core. From this it can be concluded that the mantle is mainly heated from within and, only to a minor degree, from below.

From a) and b) it follows that it is *totally improbable that the laterally averaged CMB temperature, $T_{CMB,av}$, is a constant with respect to time.* That has nothing to do with the fact that T_{CMB} should not depend on the location vector since the outer core is a metallic liquid. In spite of this consideration, convection investigations assuming a T_{CMB} which is constant with respect to time lead to good results if the considered time span is only some 100 Ma.

In Section 6.7.5, entitled Constancy of the Core-to-Mantle Heat Flux, Stacey (1992) shows that it is a better approximation for evolution models to assume a constant heat flow at CMB. Additional arguments are given by Walzer and Hendel (1999) in Appendix A. In the present model $q_{CMB} = 28.9\,mW\,m^{-2}$ is assumed using a result by Anderson (1998). Because of the paragraphs a) and b), the Rayleigh number

$$Ra = \left\langle \frac{\rho\alpha g h^3}{\kappa\eta_{al}} \cdot \frac{(Qh + q_{CMB})h}{k} \right\rangle \tag{5}$$

is better adapted to the problem than

$$Ra_B = \left\langle \frac{\rho\alpha g h^3}{\kappa\eta_{al}} \right\rangle \cdot \Delta T \tag{6}$$

The bracket $\langle\rangle$ denotes a volume average but not a temporal average. The temperature difference, $\Delta T = T_{CMB} - T_{ob}$, is no constant for the present problem, T_{ob} being the constant upper-surface temperature. The heat generation rate per volume, Q, is given by

$$Q = \rho \sum_{\nu=1}^{4} a_{\mu\nu}\, a_{if\nu}\, H_{0\nu}\, exp\,(-t/\tau_\nu) \tag{7}$$

where $a_{\mu\nu}$ is the abundance of the heat-producing elements, $a_{if\nu}$ the isotopic abundance factor, $H_{0\nu}$ the specific heat generation per unit time, $4.49 \times 10^9\,a$ ago, τ_ν the $1/e$ life of the corresponding nuclide and ν the consecutive index of the mentioned four radionuclides.

The quantity Q is monotonously declining as a function of time and also η_{al} is a function of the time since the cooling of the Earth (see paragraph a)) is an essential feature of the Earth's evolution and because of Eq. (4). Therefore, Ra is a function of time. In the main part of the time, Ra is growing less. So, steady-state models with constant Ra are not adequate to the problem. The definition

$$\log \eta_{al} = \langle \log \eta \rangle \tag{8}$$

has been used since the high values of η would dominate in a simple volume-proportional average.

3 Quantification of the model results. Non-dimensional numbers.Variation of the parameters. Conclusions.

Fig. 2 presents the temperature distribution and the creeping velocities on an equal-area projection, with constant radius, for the exponent $r_n = 0$. Similar distributions have been computed for different radii (or depths in the mantle)

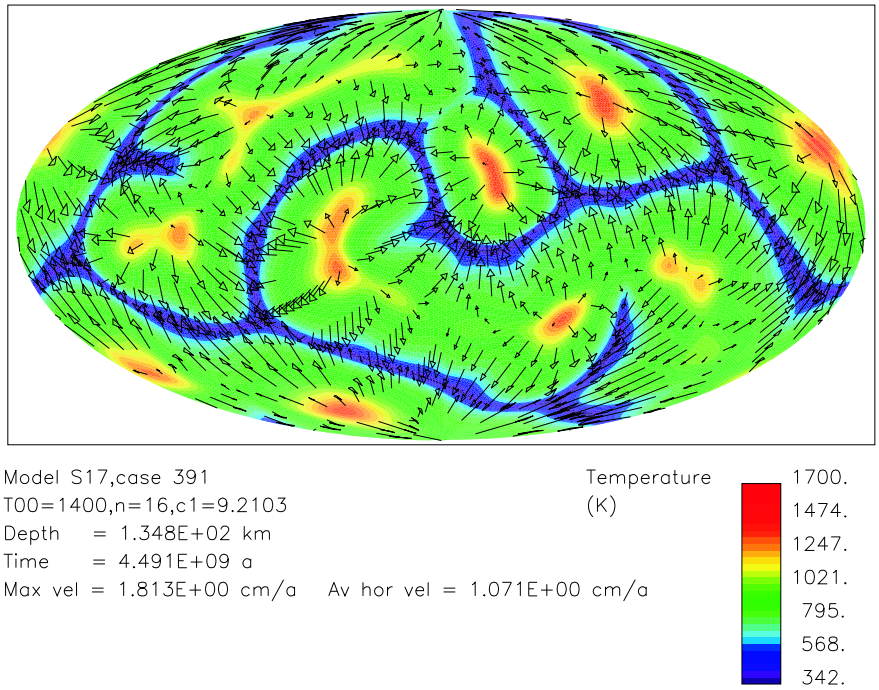

Fig. 2: Colors represent the temperature, arrows stand for the creeping velocities on an equal-area projection in 134.8 km depth. This distribution was computed by a run with Eq. (4) and $r_n = 0$ for the geological present.

and for different ages in the evolution of the system. Only non-dimensional quantities of different runs have been compared in the Figs. 3 through 9, where the systematic variation of the level of the viscosity profile was generated by the variation of r_n. Walzer et al. (2002b) investigated the influence of another temperature dependence of the viscosity on the distribution of non-dimensional quantities. If the models are more realistic, it will be difficult to discuss the mechanism since there is no simple superposition of the partial mechanisms because of non-linear relationships. To state the facts oversubtly, sometimes we have to decide whether we want to model nearer to geophysics or nearer to theoretical fluid mechanics. The mentioned papers of the authors try to bridge this gap.

Fig.3 shows the evolution of *Ra* (cf. Eq. (5)) as a function of r_n. As expected, highly viscous models evolve considerably slowly. Based on PREM and solid-state physics, our first supposition for the Earth was $r_n = 0$ (Walzer et al., 2002a). Another non-dimensional quantity, *Ror*, is represented as a function of r_n in Fig. 4. *Ror* is the *r*atio of the heat *o*utput per unit time radiated into space at the Earth's surface which stems from the Earth's in-

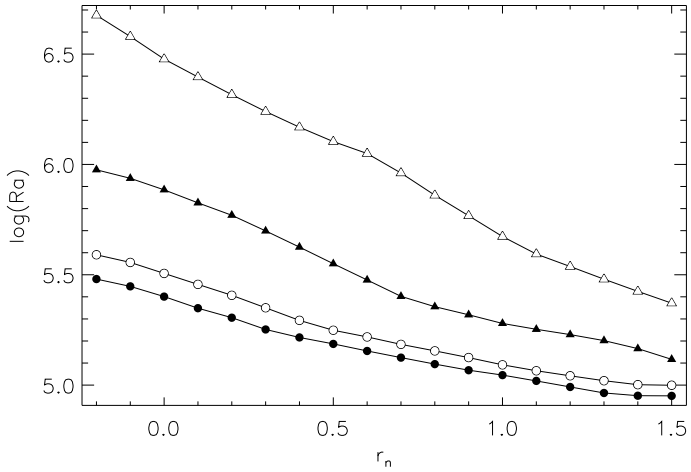

Fig. 3: The Rayleigh number, $Ra(t)$, as a function of the non-dimensional parameter r_n. Open triangles represent an age of 4000 Ma, filled triangles stand for 2000 Ma, open circles for 500 Ma, filled circles for 0 Ma.

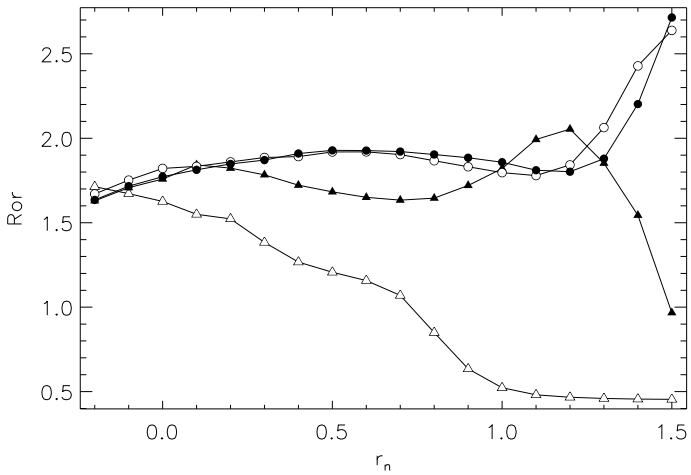

Fig. 4: The reciprocal value of the Urey number, $Ror(t)$, versus r_n. For explanation of symbols see Fig. 3.

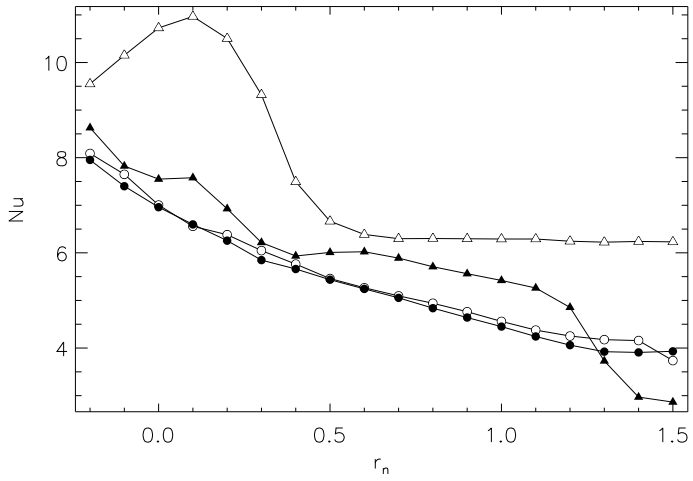

Fig. 5: The Nusselt number, $Nu(t)$, versus r_n. For explanation of symbols see Fig. 3.

terior to the *r*adiogenic heat per unit time generated in the Earth's interior. The well-known Urey number is the reciprocal value of *Ror*. We have

$$Ror = Aq/M(Q/\rho) \tag{9}$$

where all used quantities are defined above. Excluding the initial phase of the Earth's evolution with the differentiation of core and primordial mantle, the time average of *Ror* is 1.85 according to Stacey and Stacey (1999). According to Fig. 4, this requirement is fulfilled for the runs with $r_n = +0.1$ and $r_n = +0.2$, in case of wider error bars for $0.0 \leq r_n \leq +0.3$. The interval $+1.0 \leq r_n \leq +1.3$ does not give an appropriate solution since Fig. 5 shows too low Nusselt numbers for this range. For an age of 4000 Ma, the maximum Nusselt number is at $r_n = +0.1$ according to Fig. 5. This is within the most favored r_n-span and near $r_n = 0.0$ which stems from the derivation of Walzer et al.(2002a). Fig. 7 shows that the maximum of the Nusselt numbers for an age of 4000 Ma and a relative maximum of Nu for an age of 2000 Ma are situated at about $Ra(1) = 0.89 \times 10^6$. The quantity $Ra(1)$ is the Rayleigh number, Ra, defined by Eq. (5), temporally averaged over the last 4000 Ma. A comparison of the Figs. 5 and 7 demonstrates that for the low Nusselt numbers, Nu, which correspond to the interval $+1.0 \leq r_n \leq +1.3$, the relation $Ra(1) < 4 \times 10^5$ applies. Since $Ra(1) = 0.89 \times 10^6$ seems to be more realistic, this is a further reason to exclude $+1.0 \leq r_n \leq +1.3$ and higher r_n for Earth-like models. Taking no account of these strongly viscous models, Fig. 5 shows the greatest decrease in the Nusselt number during the last 4000 Ma.

Fig. 6 demonstrates the distribution of Nu versus $Ra(2)$. The latter value is the time average of Ra over the last 2000 Ma. $Ror(2)$ is defined by analogy.

$Ror(2)$ versus $Ra(2)$ is shown by Fig. 8. The realistic value of $Ror(2) = 1.85$, realistic according to Stacey and Stacey (1999), is situated somewhere in the flat maximum of Fig. 8. The relation between the temporal averages over the last 4000 Ma of Nusselt numbers and of Rayleigh numbers is depicted in Fig. 9. The exact relations to theoretical values can be checked only for a simplified mechanism. But according to tendency, the $Nu(1)$-$Ra(1)$ curve

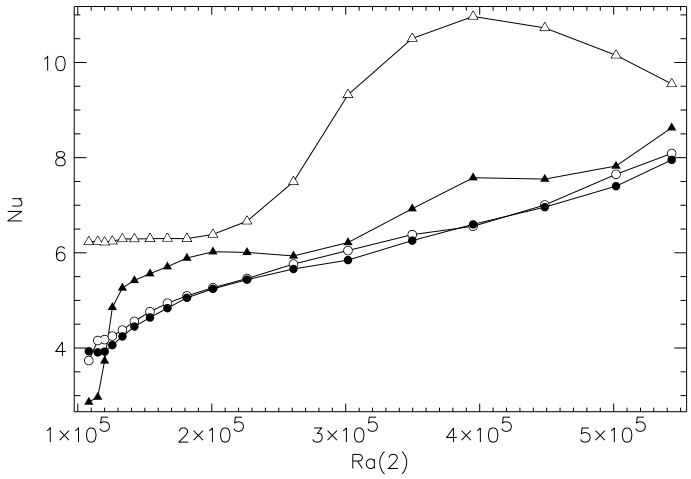

Fig. 6: The Nusselt number, $Nu(t)$, versus $Ra(2)$. The quantity $Ra(2)$ is the Rayleigh number, Ra, averaged over the last 2000 Ma. For explanation of symbols see Fig. 3.

corresponds to the usual theoretical expectations. Fig. 10 is the only picture with a dimensional quantity, namely *qob*, the heat flow in mWm^{-2}, averaged over the upper surface of the mantle. The quantity *qob* is plotted as a function of the non-dimensional r_n. The present-day mean heat flow at the Earth's surface is $87\,mWm^{-2}$, the present day mean heat flow at the upper surface of the mantle is $72\,mWm^{-2}$ according to Schubert et al. (2001). For the latter value, the contribution of the crust has been dropped. An approximate equality of the computed present-day heat flows, i.e the solid circles of Fig. 10, with the observed $72\,mWm^{-2}$ is given for $r_n = +0.1$ and $r_n = +0.2$, if somewhat larger error bars are accepted, for $0.0 \leq r_n \leq +0.3$. A second corresponding interval would be $+1.0 \leq r_n \leq +1.3$, but this second interval has to be excluded for the above mentioned reasons. Since the observed *qob* and *Ror* values stem from different information sources, this can be regarded as a confirmation that, using the interval $0.0 \leq r_n \leq +0.3$, the model produces the most Earth-like results. Further conclusions are to be found in the abstract.

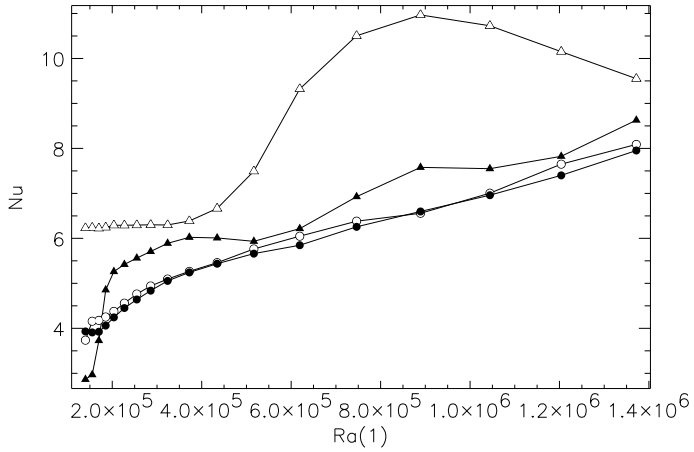

Fig. 7: Nu versus $Ra(1)$. The quantitiy $Ra(1)$ is the Rayleigh number, Ra, averaged over the last 4000 Ma. For explanation of symbols see Fig. 3.

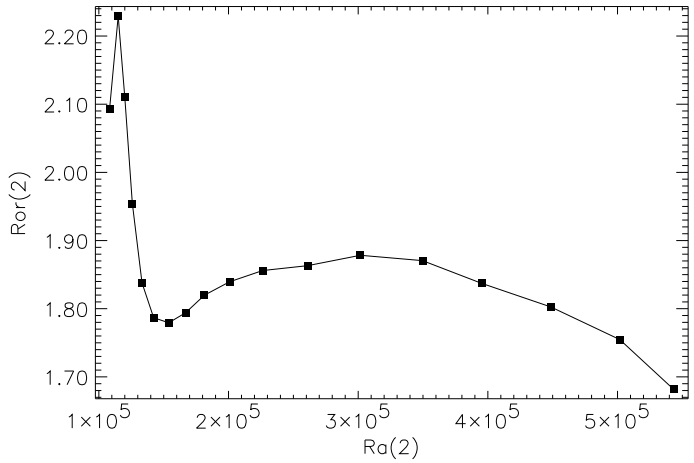

Fig. 8: $Ror(2)$ versus $Ra(2)$. The supplement (2) means the time average over the last 2000 Ma.

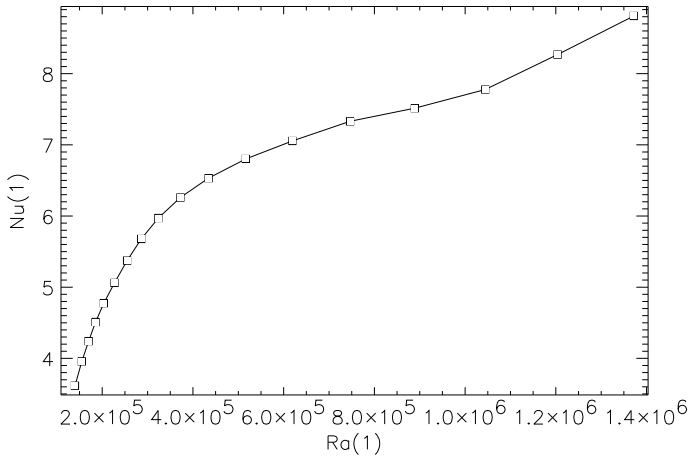

Fig. 9: The Nusselt number, $Nu(1)$, versus the Rayleigh number, $Ra(1)$. The supplement (1) stands for the time average over the last 4000 Ma.

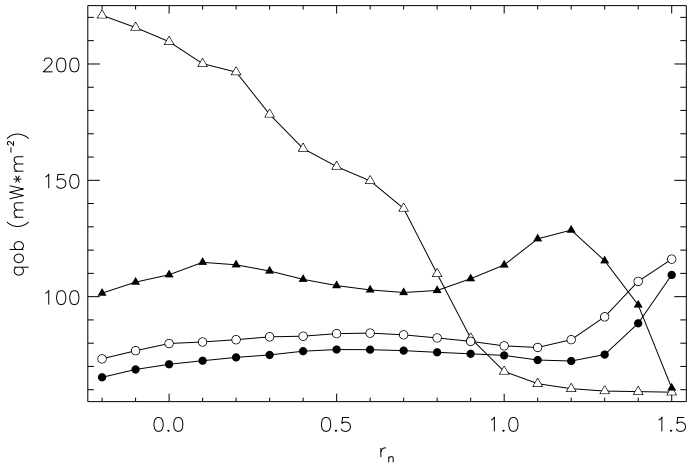

Fig. 10: The laterally averaged heat flow, $qob(t)$, at the upper surface of the spherical shell versus the non-dimensional r_n. For explanation of symbols see Fig. 3.

4 Some aspects of computing

The differential equations of convection in a compressional spherical shell are solved using a three-dimensional FE method, a fast multigrid solver and the second-order Runge-Kutta procedure. The mesh was generated by projection of a regular icosahedron onto a sphere. So, the spherical surface was divided into twenty spherical triangles or ten spherical diamonds. The successive dyadic mesh refinement procedure connects the midpoints of each side of a spherical triangle with a great circle. So, each triangle is subdivided into four smaller triangles. The radial distribution of the different spherical-surface triangular networks is so that the volumes of the cells are nearly equal. More details are given by Baumgardner (1983), Bunge et al. (1997) and Yang (1997). We used 1351746 or 10649730 grid points per run. $Ra(t)$, $Nu(t)$, $Ror(t)$ and other functions are nearly identical for runs with the different grid point numbers. For the most runs we used 128 processors on hwwt3e. The runs need 1 through 5 hours of run time. Fig 11. shows the scaling degree of the code for runs with 16, 32, 64 and 128 processors using 1351746 grid points.

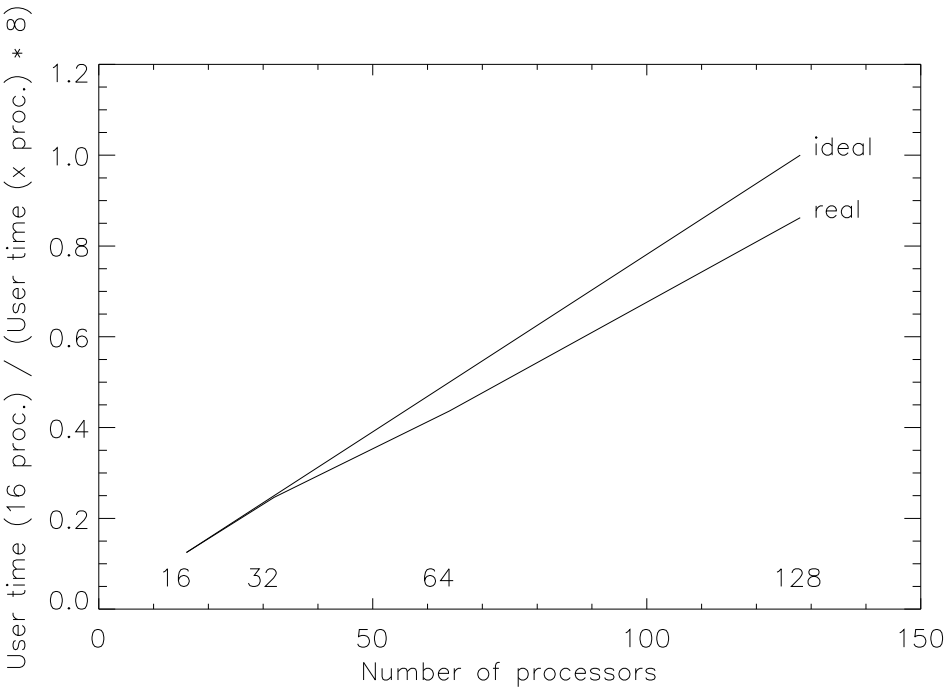

Fig. 11: Scaling degree

5 A modification of the model

If we replace Eq. (4) by

$$\eta(r,\theta,\phi,t) = 10^{r_n} \cdot \eta_1(r) \cdot exp\left[c_t \cdot T_m \left(\frac{1}{T\,(r,\theta,\phi,t)} - \frac{1}{T_{av}\,(r,t)}\right)\right] \qquad (10)$$

then we receive extremely thin slab-like downwellings. They are represented by thin blue lines in Fig. 12. The only difference between Fig. 2 and Fig. 12 is caused by the different temperature dependences (4) and (10). θ denotes the colatitude and ϕ the geographical longitude. In the lower half of the mantle, $c_t = 2$. In the upper half of the mantle, $c_t = 0$.

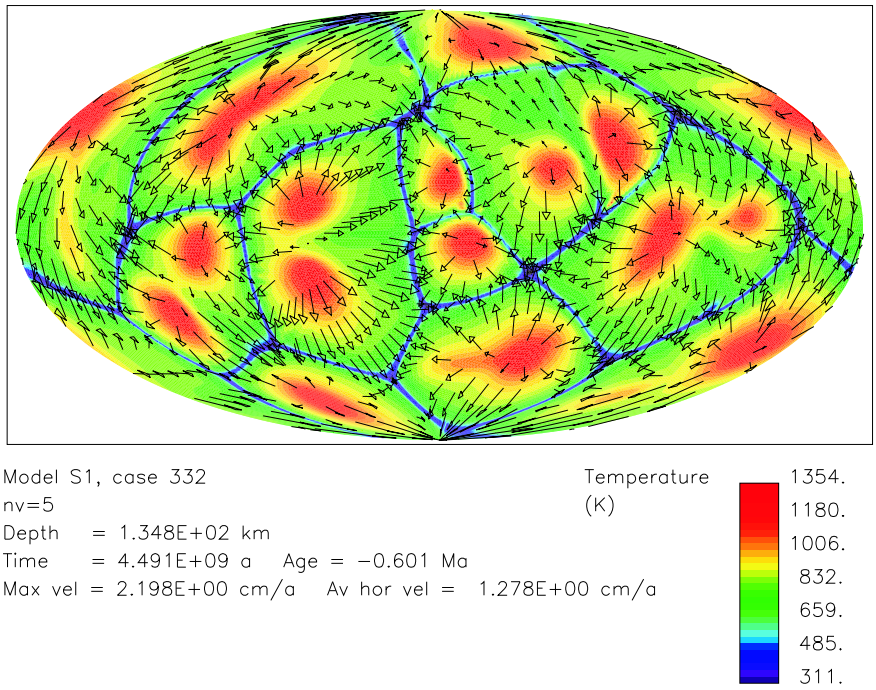

Fig. 12: Colors represent the temperature, arrows stand for the creeping velocities on an equal-area projection in 134.8 km depth. This distribution is the result of a run with Eq. (10) and $r_n = 0$ for the geological present. Although near the surface there is no plate-like distribution of the velocity arrows, the subducting downwellings (blue) are nearly slab-like. They are relatively distinct blue lines in 1350 km depth, yet, notwithstanding that a Newtonian rheology was presumed.

Acknowledgment

The provision of computer resources at the Rechenzentrum der Universität Stuttgart (HLRS) and at the John von Neumann Institute of Computing Juelich (NIC) is gratefully acknowledged.

References

Anderson, O.L., 1998. The Grüneisen parameter for iron at outer core conditions and the resulting conductive heat and power in the core. Phys. Earth Planet. Int. **109**, 179-197.

Baumgardner, J.R., 1983. A three dimensional finite element model for mantle convection. Thesis, Univ. of California, Los Angeles.

Bercovici, D., Schubert, G., Glatzmaier, G.A., 1992. Three-dimensional convection of an infinite-Prandtl-number compressible fluid in a basally heated spherical shell. J. Fluid Mech. **239**, 683-719.

Bunge, H.-P., Richards, M.A., Baumgardner, J.R., 1997. A sensitivity study of three-dimensional spherical mantle convection at 10^8 Rayleigh number: effects of depth-dependent viscosity, heating mode, and an endothermic phase change. J. Geophys. Res. **102**, 11991-12007.

Christensen, U.R., 1984. Heat transport by variable viscosity convection and implications for the Earth's thermal evolution. Phys. Earth Planet. Int. **35**, 264-282.

Christensen, U.R., 1985. Thermal evolution models for the Earth. J. Geophys. Res. **90**, 2995-3007.

Chopelas, A., Boehler, R., 1992. Thermal expansivity in the lower mantle. Geophys. Res. Lett. **19**, 1983-1986.

De Smet, J., Van den Berg, A.P., Vlaar, N.J., 2000. Early formation and long-term stability of continents resulting from decompression melting in a convecting mantle. Tectonophysics **322**, 19-33.

Ekström, G., Dziewonski, A.M., 1998. The unique anisotropy of the Pacific upper mantle. Nature **394**, 168-172.

Forte, A.M., Mitrovica, J.X., 2001. Deep-mantle high-viscosity flow and thermochemical structure inferred from seismic and geodynamic data. Nature **410**, 1049-1056.

Hofmann, A.W., 1988. Chemical differentiation of the Earth: the relationship between mantle, continental crust, and oceanic crust, Earth Planet. Sci. Lett., **90**, 297-314.

McCulloch, M.T., Bennett, V.C., 1994. Progressive growth of the Earth's continental crust and depleted mantle: Geochemical constraints. Geochim. Cosmochim. Acta **58**, 4717-4738.

Ogawa, M., 2000. Coupled magmatism-mantle convection system with variable viscosity. Tectonophysics **322**, 1-18.

Reese, C.C., Solomatov, V.S., Moresi, L.-N., 1999. Non-Newtonian stagnant lid convection and magmatic resurfacing on Venus. Icarus **139**, 67-80.

Safronov, V.S., 1972. Evolution of the Protoplanetary Cloud and Formation of the Earth and Planets. Nauka, Moscow. Translation by the Israel Program for Scientific Translation.

Schmalzl, J., 1996. Mixing properties of thermal convection in the Earth's mantle. Geologica Ultraiectina, no. 140

Schubert, G., Cassen, P., Young, R.E., 1979. Subsolidus convective cooling histories of terrestrial planets. Icarus **38**, 192-211.

Schubert, G., Stevenson, D., Cassen, P., 1980. Whole planet cooling and the radiogenic heat source contents of the Earth and Moon. J. Geophys. Res. **85**, 2511-2518.

Schubert, G., Turcotte, D.L., Olson, P., 2001. Mantle Convection in the Earth and Planets. Cambridge Univ. Press, Cambridge, 940 pp.

Solomatov, V.S., 1995. Scaling of temperature- and stress-dependent viscosity convection. Phys. Fluids **7**, 266-274.

Spohn, T., Schubert, G., 1991. Thermal equilibrium of the Earth following a giant impact. Geophys. J. Int. **107**, 163-170.

Stacey, F.D., 1992. Physics of the Earth, 3rd edn., Brookfield Press, Brisbane, 513 pp.

Stacey, F.D., Stacey, C.H.B., 1999. Gravitational energy of core evolution: Implications for thermal history and geodynamo power. Phys. Earth Planet. Int. **110**, 83-93.

Walzer. U., Hendel, R., 1999. A new convection-fractionation model for the evolution of the principal geochemical reservoirs of the Earth's mantle. Phys. Earth Planet. Int. **112**, 211-256.

Walzer. U., Hendel, R., 2002. Chemical differentiation, viscosity and the thermal evolution of the mantle. Pure Appl. Geophysics, in press.

Walzer. U., Hendel, R., Baumgardner, J., 2002a. A 3–D compressible spherical-shell model of the thermal evolution of the Earth's mantle. Tectonophysics, in press.

Walzer. U., Hendel, R., Baumgardner, J., 2002b. A sensivity study of a 3–D compressible spherical-shell model of mantle convection. Earth Planet. Sci. Lett., in press.

Yang, W.-S., 1997. Variable viscosity thermal convection at infinite Prandtl number in a thick spherical shell. Thesis, Univ. of Illinois, Urbana-Champaign.

Zhang, S., Yuen, D.A., 1996. Various influences on plumes and dynamics in time-dependent, compressible mantle convection in 3–D spherical-shell. Phys. Earth Planet. Int. **94**, 241-267.